

# Infrared technique for measuring thickness of a flowing soap film

Cite as: Review of Scientific Instruments **72**, 2467 (2001); <https://doi.org/10.1063/1.1366634>

Submitted: 07 November 2000 • Accepted: 19 February 2001 • Published Online: 24 April 2001

X. L. Wu, R. Levine, M. Rutgers, et al.



View Online



Export Citation

## ARTICLES YOU MAY BE INTERESTED IN

[Measuring soap bubble thickness with color matching](#)

American Journal of Physics **79**, 1079 (2011); <https://doi.org/10.1119/1.3596431>

[The slowest soap-film tunnel in the Southwest](#)

Review of Scientific Instruments **73**, 1177 (2002); <https://doi.org/10.1063/1.1446040>

[Conducting fluid dynamics experiments with vertically falling soap films](#)

Review of Scientific Instruments **72**, 3025 (2001); <https://doi.org/10.1063/1.1379956>

Lock-in Amplifiers  
up to 600 MHz



Zurich  
Instruments



# Infrared technique for measuring thickness of a flowing soap film

X. L. Wu<sup>a)</sup> and R. Levine

*Department of Physics and Astronomy, University of Pittsburgh, Pittsburgh, Pennsylvania 15260*

M. Rutgers

*Department of Physics, The Ohio State University, Columbus, Ohio 43210*

H. Kellay

*Centre de Physique Moléculaire Optique et Hertzienne, Université Bordeaux I, 351 Cours de la Libération, 33405 Talence Cedex, France*

W. I. Goldberg

*Department of Physics and Astronomy, University of Pittsburgh, Pittsburgh, Pennsylvania 15260*

(Received 7 November 2000; accepted for publication 19 February 2001)

In conducting two-dimensional laminar and turbulence experiments, use of a vertical flowing soap film is often a good choice. However, one of the most frequently encountered and yet highly nontrivial problems is to measure the thickness of the film precisely. We propose a solution to this problem based on the strong absorption of infrared light by the water molecules in the film. At  $\lambda \approx 3 \mu\text{m}$ , a thin sheet of water is essentially opaque. The extinction length of  $0.9 \mu\text{m}$  serves as a precise ruler for gauging the film thickness. Although only the time-averaged, single-point measurements are presented, the technique is general and can be used for multipoint measurements to investigate turbulent driven spatiotemporal fluctuations of the film thickness. © 2001 American Institute of Physics. [DOI: 10.1063/1.1366634]

## I. INTRODUCTION

There is current interest in using soap films to conduct laboratory fluid mechanics experiments.<sup>1</sup> This interest stems from the small thickness of these films, making them good candidates for studying fluid flows and turbulence in a nearly two-dimensional (2D) geometry. For the 2D approximation to be valid, a crucial assumption is that the soap film thickness is uniform, so that its density  $\rho_2 = \rho h$  remains constant during flow. Here  $\rho = 1 \text{ g/cm}^3$  is the density of water and  $h$  is the film thickness. If quantitative work is required, it is also important to know the viscosity of the 2D fluid, which has been found to vary inversely with film thickness  $h$  and thus has a strong  $h$  dependence for thin films.<sup>2-4</sup>

Casual observations of soap films or bubbles show intricate striations and beautiful colors, suggesting that inhomogeneities in these films are of the order of a visible wavelength. In a recent experiment, we have constructed a 2D channel, with  $h$  and other parameters under experimental control.<sup>5,6</sup> The apparatus has since been used by several research groups to conduct 2D fluid flow and turbulence experiments.<sup>5-8</sup> Even under such an idealized condition, color fringes are still discernible. There remains an urgent need to characterize these inhomogeneities and to evaluate their dynamic significance for 2D fluid flows.

At first glance the film thickness measurement appears to be trivial, since there are many standard techniques for measuring the thickness of thin films. For instance, optical reflectivity and ellipsometry are routinely used in laboratories for characterizing thin solid and fluid films. However, we found

that these standard techniques are not adequate for soap films moving with speeds which are often in excess of several meters per second. This is because soap films are fluids; once they are set in motion there is always a small, yet finite, out-of-plane fluctuation that causes an unsteady reflected light beam, which makes the standard types of measurement impossible. Alternatively, one may use the interference fringes to measure the film thickness.<sup>9</sup> However, such a technique can only yield a relative change in thickness, not its absolute value, unless the order of the interference fringes can be enumerated. This sometimes turns out to be not feasible.

To overcome these difficulties we have devised an infrared (IR) absorption technique to measure  $h$ . Since the measurement relies on light transmission, the technique is much less susceptible to out-of-plane fluctuations of the film. The optical technique achieves its high sensitivity by means of a remarkable IR absorption property of water molecules, which make up 99% of the soap solution. Specifically, it is well established that, at a wavelength  $\lambda \approx 3 \mu\text{m}$ , a thin layer of water is essentially opaque to such a radiation with an extinction length  $z_0 \approx 0.9 \mu\text{m}$ . This extinction length is even smaller than the typical film thickness used in most of our experiments.<sup>3,5,6</sup>

In Sec. II, we describe the experimental setup and estimate the spatial and temporal resolution of the local thickness  $h(x, y; t)$ . In Sec. III we present measurements of the time-averaged thickness profiles along the direction of mean flow and perpendicular to it for both laminar and turbulent flows in the soap film channel. In Sec. IV we speculate about possible improvements to the current setup and its potential use for the study of passive-scalar turbulence.

<sup>a)</sup>Electronic mail: xlwu+@pitt.edu

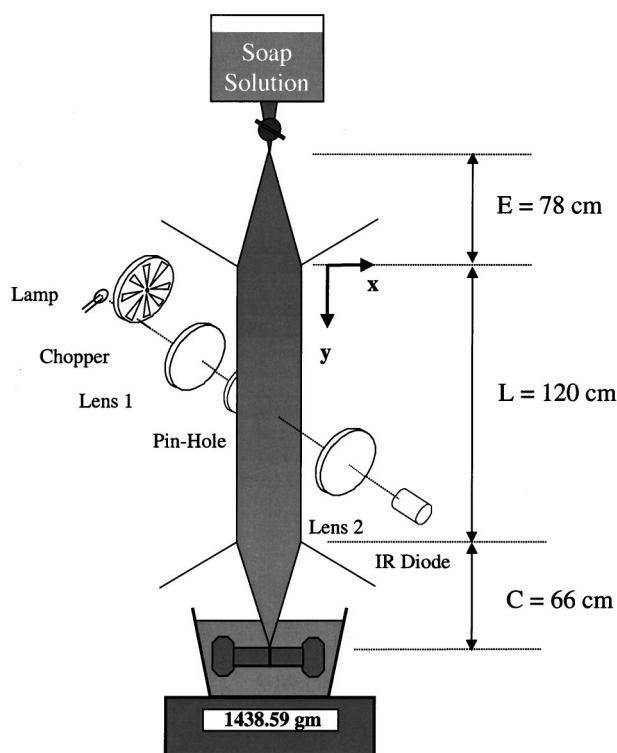


FIG. 1. IR setup consisting of an IR light source (a 0.5 W incandescent lamp with a small filament), an optical chopper, a set of IR lenses, a pinhole, a narrow band-pass filter ( $3.0 \pm 0.1$ ), and a two-stage cooled InAs photodetector. The chopped signal is measured by a lock-in amplifier. At its ends, the flowing soap film channel has an upper and a lower reservoir. The upper reservoir is maintained at constant hydrostatic pressure using a magnetically coupled gear pump. This ensures a constant injection rate, which replenishes the soap film in the channel. The flow speed is controlled by a valve located above the plastic nozzle as shown. The border of the film is formed by two nylon strings (diameter=0.5 mm) that are held taut by a weight submerged in the lower reservoir. These strings are kept parallel by a set of four pulling strings (diameter=0.1 mm) and maintained at a constant width of  $W = 5$  cm. The overall flow rate is measured directly using a digital balance, and velocity measurement is carried using a LDV. Turbulence in the film is created by inserting a grid perpendicular to the flow.

## II. EXPERIMENTAL DESCRIPTION

### A. IR optics and detection

Shown in Fig. 1 is our experimental setup along with the 2D soap film channel, which will be discussed briefly later. The optical train consists of the following components: an IR light source (a small incandescent lamp), an optical chopper (Stanford Research Systems, model SR540), a set of IR lenses, a pinhole, and a narrow band-pass filter ( $3.00 \pm 0.01 \mu\text{m}$ , Oriel Instruments) located in front of a photodetector. The detector is a two-stage cooled InAs diode (EG&G Judson, model J12TE2-BB6-R01M), which operates at  $-40^\circ\text{C}$  to minimize the thermal noise. The optical alignment is relatively straightforward. A sharp image of the lamp filament is projected onto the soap film plane using lens 1, and an aperture (diameter=0.20 mm) is used to limit the illumination area. The transmitted light is refocused onto the photodetector using lens 2.

An important consideration of the optical design is the transmitted IR beam profile. This essentially determines the spatial resolution of our instrument; for many practical rea-

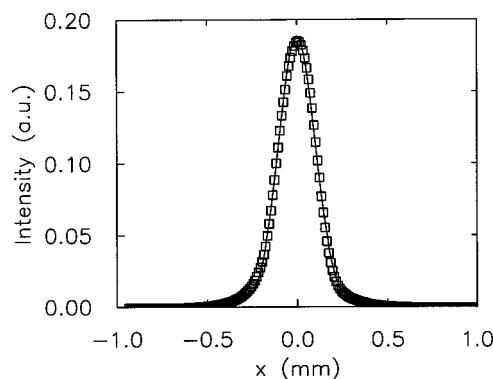


FIG. 2. IR beam profile. The measurement was carried out by scanning a thin slit across the incident IR beam near the surface of the flowing soap film. The solid line is a Lorentzian fit.

sons, it should be small. We attempted to measure the IR beam profile in the  $x$  direction by translating a narrow slit (0.05 mm) in front of the soap film. For a slit width that is much smaller than the diameter of the beam, which is determined by the size of the pinhole, the half height full width  $\sigma$  of the transmitted intensity distribution gives a quantitative measure of the diameter of the IR beam. As seen in Fig. 2, the transmission intensity profile can be fitted quite satisfactorily by a Lorentzian (see the solid line) with the width  $\sigma \approx 0.19$  mm, which is comparable to the size of the pinhole used. By making  $\sigma$  small, we increase the spatial resolution at the expense of reducing the overall intensity of the incident IR beam. To detect the weak intensity, we relied on a phase lock-in technique by chopping the input light at a frequency of 4 kHz. The transmitted light is fed to a lock-in amplifier (EG&G, model 5209) with a low-pass filter of 1 kHz. Thus, the instrument we built essentially has a spatial resolution of 0.2 mm and a temporal resolution of  $\sim 1$  ms.

At a normal incidence, the transmitted light intensity  $I_T$  depends on  $h$  and  $z_0$  and can be calculated by taking into account multiple reflections of beams from liquid-air interfaces. A simple calculation showed that the transmittance is given by

$$T = \frac{I_T}{I_0} = \frac{(1-R)^2 e^{-h/z_0}}{1-R^2 e^{-2h/z_0}}, \quad (1)$$

where  $I_0$  is the incident light intensity, and  $R$  is the reflectance given by  $R = (n-1)^2/(n+1)^2$  with  $n$  being the index of refraction of water. At  $\lambda = 3 \mu\text{m}$ ,  $n = 1.17$  for a water/air interface yielding  $R \approx 0.61\%$ , which is very small. To a good approximation, therefore, the transmittance  $T$  decays exponentially with the film thickness, i.e.,  $T = \exp(-h/z_0)$ , making the data analysis simpler. For completeness, in Fig. 3 we show  $z_0$  as a function of  $\lambda$  in the IR regime for water.<sup>10</sup> Note that, at  $\lambda = 3.0 \mu\text{m}$ , water has a sharp absorption peak with  $z_0 \approx 0.9 \mu\text{m}$ . The smallness of  $z_0$  makes the technique very sensitive to minor changes in soap film thickness  $h$ . The dependence of  $z_0$  on  $\lambda$  also makes the technique flexible in detecting thicker films by shifting  $\lambda$  to a shorter or longer wavelength.

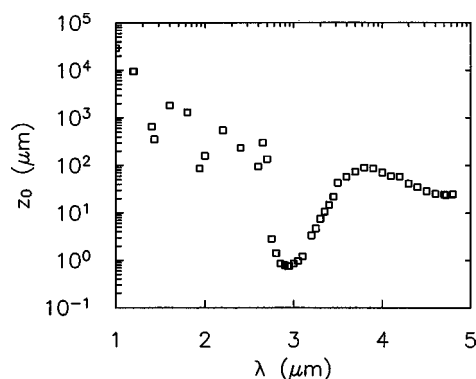


FIG. 3. Infrared absorption curve for water. Notice a sharp decrease of  $z_0$  at about  $3\ \mu\text{m}$  wavelength.

## B. 2D soap film channel

Details of the experimental setup for the soap film channel was described in an earlier publication.<sup>5,6</sup> Briefly, the channel is formed by two nylon wires, 0.5 mm in diameter, as illustrated in Fig. 1. At the top of the channel, the two wires converge to a single point that is attached to a plastic nozzle. The wires at the bottom are tied to a 1 kg weight, which is submerged in a lower reservoir. The soap solution is injected from the top and is recirculated via a magnetically driven pump. The injection rate is regulated by a metering valve and measured by an electronic balance underneath the lower reservoir. To initiate a film, the two vertical wires are pinched together and the soap solution drips along the wires. When the entire length of the wires is wetted by the soap solution, the wires are separated by a set of four pulling wires, as shown in Fig. 1. The film thus formed slides down due to gravity, and its velocity is determined by the injection rate and the channel width  $W$ , which was set to 5 cm for all the measurements. Since the film is continuously replenished at the top, the flow is stable and can last for many hours. The soap solution used in this experiment is 1% liquid detergent (Dawn) and 99% distilled water. Small polystyrene spheres (diameter =  $1\ \mu\text{m}$ ) are added to the soap solution to facilitate velocity measurements by a laser Doppler velocimeter (LDV).

## III. EXPERIMENTAL MEASUREMENTS

In the following we present thickness measurements of a flowing soap film in the test section of the channel. As shown in Fig. 1, the test section spans a distance from  $y=0$  to 120 cm with a width of 5 cm.

### A. Thickness profiles in laminar flows

In a laminar flow, the injection rate and the width of the channel determine the thickness profiles both along the flow and perpendicular to it. This is because any inhomogeneity created by the injection nozzle takes time to relax. If one considers that the thickness variations are passively transported by the mean flow, it follows that the inhomogeneities take a shorter distance to anneal the slower is the mean flow. This is what has been observed. The relaxation of the film thickness towards a uniform distribution is somewhat like diffusion of a dye in a flow, except here the rate of relaxation

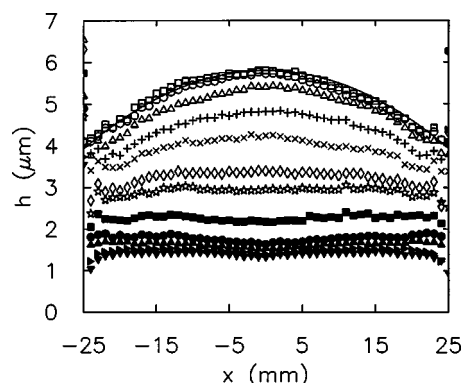


FIG. 4. Horizontal thickness profiles in the laminar flow regime. The measurements were carried out at  $y=70\ \text{cm}$  from the entrance point. A wide range of injection rates  $J$  was used. In the increasing order of film thickness, the following  $J$  values were used in the measurement:  $J=0.041, 0.054, 0.089, 0.119, 0.204, 0.303, 0.385, 0.513, 0.645, 0.769, 0.833$ , and  $1.00\ \text{g/s}$ . The statistical uncertainty is comparable to the size of the symbols used.

is determined by the surface tension rather than by diffusion.<sup>9</sup> Thus by measuring how fast the thickness profile evolves, one can obtain useful information about the surface tension and elasticity of the film.

The first set of measurements were carried out at a fixed distance ( $y=70\ \text{cm}$ ) from the entrance. The thickness profile transverse to the mean flow,  $h(x)$ , was measured as a function of the injection rate  $J$ . As can be seen in Fig. 4, there is a marked change in the shape of  $h(x)$  as  $J$  is increased. For low injection rates,  $0.04 < J < 0.39\ \text{g/s}$ , the film thickness is essentially uniform in the center region of the channel but decreases slightly near the bounding wires. The thinning of the film near the border at small  $J$  is rather surprising considering that the diameter of the wires is orders of magnitude greater than the mean-film thickness. Naively one would expect that soap solution tends to flow along the wires making the film thicker near the wires than away from them. This is clearly not the case. However, this phenomenon is consistent with the observation that, for very low injection rates,  $J < 0.04\ \text{g/s}$ , thin patches of black films are constantly nucleated near the bounding wires, and buoyancy can lift them up against the background flow. If the thin patches are not promptly flushed out of the channel, they grow in size and eventually cause the film to break. This phenomenon, so called marginal regeneration, was first studied by Mysels *et al.*<sup>1</sup> and is a result of the negative Laplace pressure created in the film when it is attached to a thicker border. What is unusual in our experiment is that, even in the presence of the flow, the negative pressure is still seen to exert its influence on the thinning of the film.

As  $J$  increases,  $0.4 < J < 1.0\ \text{g/s}$ , the thickness in the center builds up rapidly and, to a good approximation, the shape of the profile can be described by a parabolic function, shown as a solid line in the graph. Even for these rather large injection rates, the thickness near the boundaries is still smaller than in the center of the channel. The above measurements demonstrate that, for a laminar flowing soap film, a reasonably uniform film thickness can be achieved in the center of the channel ( $-20 < x < 20\ \text{mm}$ ) for a wide range of



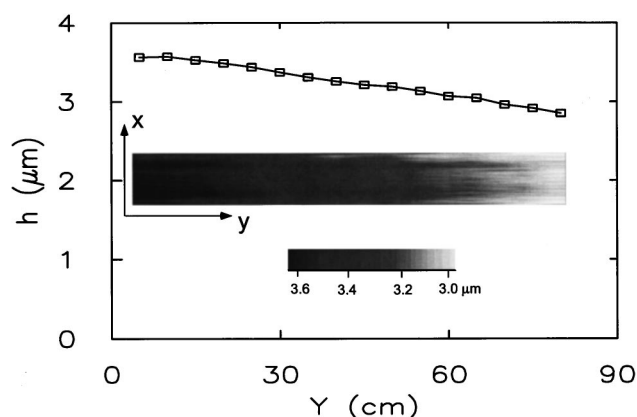


FIG. 5. Thickness map measured with  $J=0.303$  g/s fixed. The film is thicker at the top and thinner at the bottom, suggesting stretching of the film as it accelerates downstream. The thickness variation is  $\approx 0.6$   $\mu\text{m}$  over  $\sim 80$  cm in the vertical direction, and  $0.1$   $\mu\text{m}$  in the horizontal direction.

injection rates  $0.04 < J < 0.4$  g/s. The fractional variation  $\delta h/h$  in that region is well under 10%.

Measurements such as those in Fig. 4 can be repeated for different heights  $y$  for a given injection rate. This is shown in Fig. 5 for  $J=0.303$  g/s. The plot is coded by gray scales with darker and lighter tones indicating thick and thin regions, respectively. It is seen that near the entrance  $h$  is  $3.6$   $\mu\text{m}$  and that it decreases to  $2.9$   $\mu\text{m}$  at  $y=80$  cm downstream. The thickness thus changes by  $\sim 20\%$  throughout the length of the channel, while the variations in the transverse direction decrease steadily at different heights downstream.

We also carried out measurements of the vertical thickness profile along the centerline for different injection rates  $J=0.172, 0.303, 0.476$ , and  $0.714$  g/s. This is plotted in Fig. 6. We noted that as  $J$  increases, the average film thickness increases and, at the same time, there is a gradual change of the thickness gradient  $dh/dy$ , varying from  $0.4$  to  $0.8$   $\mu\text{m}/\text{m}$  for low to high injection rates. The presence of this thickness gradient is a result of a residual acceleration of the film, which causes the film to stretch along the flow. This also suggests that, for rates greater than  $J \approx 0.2$  g/s (or  $h > 3$   $\mu\text{m}$ ), a truly steady-state flow cannot be reached with the current apparatus. Achieving a high velocity with a steady-state flow is important for many 2D experiments; it can be realized

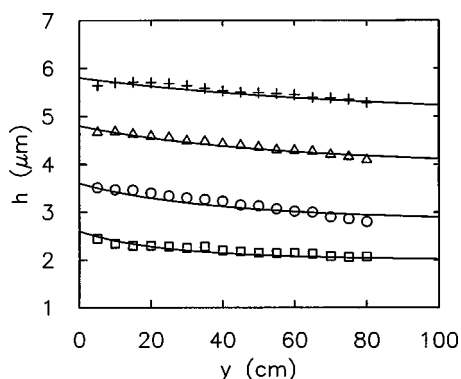


FIG. 6. Vertical thickness profiles along  $x=0$  for different injection rates:  $J=0.172, 0.303, 0.476$ , and  $0.714$  g/s, corresponding to squares, circles, triangles, and crosses, respectively. The solid lines are guides to the eyes.

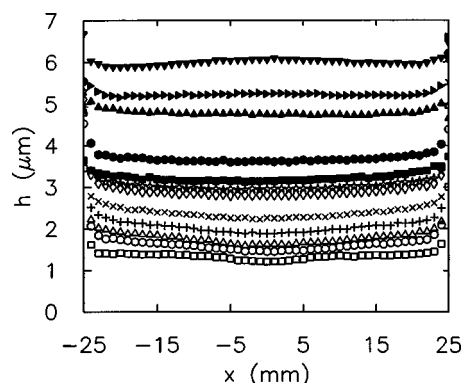


FIG. 7. Horizontal thickness profiles in the turbulent flow regime. The measurements were carried out at  $y=30$  cm from the entrance point. A wide range of injection rates  $J$  was used. In the increasing order of film thickness, the following  $J$  values were used:  $0.063, 0.083, 0.098, 0.125, 0.167, 0.217, 0.244, 0.270, 0.330, 0.556, 0.690$ , and  $1.177$  g/s in the measurement. Compared to Fig. 4, it is evident that the film thickness is more uniform in the turbulent flow regime than in the laminar regime. The statistical uncertainty is comparable to the size of the symbols used.

only for soap films much longer in length than those in our current setup.<sup>6</sup>

## B. Thickness profiles in turbulent flows

We also measured the film thickness profiles in turbulent flowing soap films. Here turbulence is generated by a grid (a comb with  $1$  mm diam teeth and  $2$  mm spacing between the teeth) placed at  $y=1.5$  cm below the entrance level. The measurement itself was carried out  $24$  cm below the grid. Figure 7 shows the time-averaged horizontal thickness profiles as a function of  $J$ . In contrast to Fig. 4, the measurements here clearly indicate that  $h$  is essentially independent of the horizontal position  $x$  even for  $J$  as large as  $1.2$  g/s. It is evident that grid generated turbulence efficiently homogenizes the thickness in the channel. However, if one measures the root-mean-square (rms) fluctuations of  $h$ , one finds that  $h_{\text{rms}}$  increases with  $J$ , as seen in Fig. 8. It is also clear from Fig. 8 that for most  $J$  values,  $h_{\text{rms}}$  in the presence of turbulence (shown by squares) is nearly a factor of 2 greater than that measured in the laminar flow (shown by circles). For the highest injection rate,  $J \approx 1.17$  g/s,  $h_{\text{rms}}$  levels off (see

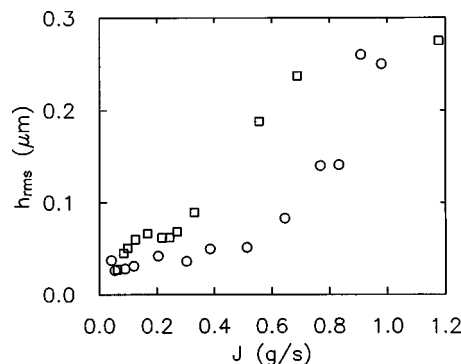


FIG. 8. Root-mean-square thickness fluctuations in grid turbulence (squares). For a comparison, the same measurement in the laminar flow regime is also displayed (circles). As seen, as the injection rate  $J$  increases, so does the rms fluctuations of the thickness. Overall, the  $h_{\text{rms}}$  in the turbulent regime is almost twice as large as that in the laminar regime.

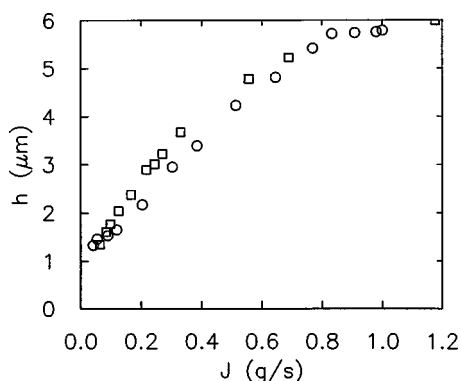


FIG. 9. Mean thickness vs injection rate. For comparison, we also plot both measurements carried out in the turbulence regime (squares) and in the laminar flow regime (circles). Both measurements were carried out at  $y \approx 25$  cm.

Fig. 8) due to the finite integration time in the thickness measurement, showing that significant thickness fluctuations occur on time scales shorter than the 1 ms set by the lock-in amplifier. However, for moderate injection rates of  $J \approx 0.4$  g/s and below (corresponding to  $h \leq 4$   $\mu\text{m}$ ), the measurements are unaffected by the time constant of the lock-in amplifier and  $h_{\text{rms}}/h < 5\%$ , which is rather small.

A notable finding of our measurements is that the relationship between  $h$  and  $J$  depends on whether flow is laminar or turbulent, as shown in Fig. 9. Here we find that, in the presence of the grid, the mean film thickness is larger than in the laminar flowing film when  $J > 0.1$  g/s, despite the fact that for small flow rates,  $J < 0.1$  g/s, the two measurements are nearly identical. The behavior for large injection rates may be understood as follows. In the presence of the grid, a significant amount of kinetic energy in the mean flow is transferred to turbulent velocity fluctuations, resulting in a lower mean speed than in the corresponding laminar flow case. The conservation of the mass flux  $J = Wh\rho v$  therefore dictates that the average film thickness and the average velocity must be correlated, i.e., for  $J$  fixed, a higher mean velocity implies a thinner film. In principle, the presence of the grid turbulence can also cause mixing which can enhance diffusion of surfactants in and out of the surface layers in the soap film, resulting in a change of the surface properties of the soap film. How such a change will affect the flow is interesting but is not clear at present.

#### IV. DISCUSSION

We have developed a simple and robust means of measuring the thickness of a fast moving soap film. This technique allows one, for the first time, to accurately characterize

the film thickness profiles in a 2D channel. Our measurements show that, due to the presence of gravity, the film changes its thickness in the vertical direction and a constant film thickness ( $dh/dy = 0$ ) or, equivalently, a constant velocity, is achieved in laminar flow only for injection rate  $J$  less than 0.2 g/s. For large injection rates, a much longer channel is required in order to reach the terminal thickness (or velocity). Our measurements also show that, even in the turbulent regime, the root-mean-square thickness fluctuation is only 5% of the mean thickness. This is consistent with particle imaging velocimetry measurements, which show the root-mean-squared divergence of the turbulent flow in the soap film is 10% for films as thick as 30–50  $\mu\text{m}$ .<sup>7,11</sup>

Currently there is considerable interest in scalar turbulence.<sup>12</sup> It has been speculated that, in flowing soap films, small thickness variations  $\delta h(x, y)$  are passively advected by the velocity field and thus behave like a passive scalar, similar to a dye or temperature.<sup>9,13</sup> The technique reported here is well suited for studying statistical fluctuations of  $\delta h(x, y)$  in 2D turbulence. To fully reach its potential, with a higher spatiotemporal resolution, a brighter and better collimated IR source is needed. Certain solid-state diode laser appear to be able to tune to 3  $\mu\text{m}$  wavelength. However, a more practical way perhaps is to equip a high-power HeNe laser with special optics. The HeNe laser is known to emit IR radiation at 3.39  $\mu\text{m}$  with high efficiency. The technique reported here would also help to solve an array of outstanding questions concerning rheological properties of flowing soap films.

#### ACKNOWLEDGMENT

This research was supported by grants from NSF and from NASA.

- <sup>1</sup>K. J. Mysels, K. Shinoda, and S. Frankel, *Soap Films, Studies of Their Thinning* (Pergamon, New York, 1959).
- <sup>2</sup>A. A. Trapeznikov, *Proceedings of the Second International Congress of Surface Activity* (Academic, New York, 1957), p. 242.
- <sup>3</sup>B. Martin and X. L. Wu, *Rev. Sci. Instrum.* **66**, 5603 (1995).
- <sup>4</sup>P. Vorobieff and R. E. Ecke, *Phys. Rev. E* **60**, 2953 (1999).
- <sup>5</sup>H. Kellay, X. L. Wu, and W. I. Goldburg, *Phys. Rev. Lett.* **74**, 3975 (1995).
- <sup>6</sup>M. Rutgers, X. L. Wu, R. Bhagavatula, A. A. Petersen, and W. I. Goldburg, *Phys. Fluids* **8**, 2847 (1996).
- <sup>7</sup>M. Rivera, P. Vorobieff, and R. E. Ecke, *Phys. Rev. Lett.* **81**, 1417 (1998).
- <sup>8</sup>J. Zhang, S. Childress, A. Libchaber, and M. Shelley, *Nature (London)* **408**, 835 (2000).
- <sup>9</sup>X. L. Wu, B. Martin, H. Kellay, and W. I. Goldburg, *Phys. Rev. Lett.* **75**, 236 (1995).
- <sup>10</sup>V. M. Zolotarev, B. A. Mikhailov, L. L. Alperovich, and S. I. Popov, *Opt. Spectrosc.* **27**, 430 (1969).
- <sup>11</sup>M. Rivera and X. L. Wu, *Phys. Rev. Lett.* **85**, 976 (2000).
- <sup>12</sup>B. I. Shraiman and E. D. Siggia, *Nature (London)* **405**, 639 (2000).
- <sup>13</sup>J. M. Chomaz and B. Cathalau, *Phys. Rev. A* **41**, 2243 (1990).